Dynamic stability of Time-Delayed Feedback Control System by FFT based IHB Method

R. K. MITRA
Department of Mechanical Engineering
National Institute of Technology, Durgapur (Deemed University)
West Bengal, Pin-713209
INDIA
rkmitra.me@gmail.com, http://www.nitdgp.ac.in/faculty_details.php?id=122

A. K. BANIK
Department of Civil Engineering
National Institute of Technology, Durgapur (Deemed University)
West Bengal, Pin-713209
INDIA
akbanik@gmail.com, http://www.nitdgp.ac.in/faculty_details.php?id=21

S. CHATTERJEE
Department of Mechanical Engineering
Bengal Engineering and Science University, Shibpur
West Bengal, Pin-711103
INDIA
shychat@gmail.com, http://www.becs.ac.in/aboutshyamal-chatterjee-mech-menuitem

Abstract: - The forced Duffing oscillator is investigated by intentional time-delayed displacement feedback by fast Fourier transform based incremental harmonic balance method along with continuation technique (FFT-IHBC). FFT-IHBC can efficiently develop frequency response curves with all stable and unstable solutions and solution branches. Appreciable reduction in peak value of response and gradual reduction in the skew-ness in frequency response curve is observed with the introduction of gain and delay. Further, frequency response curves with all stable solutions can be achieved with appropriate choice of gain and delay in the primary and secondary stability zones of linear stability analysis. The results obtained by this method are compared with numerical integration method and they match perfectly.

Key-Words: - Fast Fourier transform; incremental harmonic balance method; are length continuation; intentional time-delayed feedback; Floquet stability.

1 Introduction

Controlling resonant vibrations of flexible machine components and structural members has always been an important area of research for engineers. In the past various methods analytical, semi-analytical and numerical methods were available for controlling resonant vibrations. Though active vibration control is a superior to passive control techniques, presence of unavoidable time delays in the feedback circuit seriously limits the performance of an active control system and in the worst case the system response may even become unbounded. Thus, it is extremely difficult to meet the desire objectives of vibration control systems under the presence of uncontrollable time-delay. The common mathematical methods available for the analysis of the aforesaid class of systems is the method of Multiple Time Scales (MTS) and straight forward harmonic balance (HB) analysis. But such methods works well only for weakly non-linear systems and for time-delays smaller compared to the natural time period of vibration of the system. A comprehensive survey of the recent research on the field is available in [1].

Olgac et al. [2, 3] have developed an active vibration absorber based on linear time-delayed

state feedback, which they have termed as the delayed resonator. Hu et al. [4] have reported time-delayed state feedback control of the primary and 1/3 sub-harmonic resonances of a forced Duffing oscillator. Udwadia et al. [5 to 7] have investigated the application of time-delayed velocity feedback for controlling the vibrations of structural systems under seismic loading. Maccari [8] and Atay [9] have studied vibration control of self-excited systems. The primary resonance of a cantilever beam under the time-delayed feedback control has been studied by Maccari [10]. Chatterjee [11] have discussed time-delayed feedback control of various friction-induced instabilities. Vibration control by recursive time-delayed acceleration feedback has also been studied by Chatterjee [12]. Ram et al. [13] consider the eigenvalue assignment problem for a linear vibratory system using state feedback control in the presence of time-delay. El-Bassiouny and El-kholy [14] present analytical and numerical studies on the effect of time-delayed feedback of a non-linear SDOF system under external and parametric excitations.

As stated earlier, presence of unavoidable time delays in the feedback circuit seriously limits the performance of an active control system by destabilizing it at high control gains. In order to circumvent this undesirable situation, time-delay is intentionally introduced in the feedback path where, the gain and the time-delay are both controllable. Further, literature survey reveals that studies on the effect of intentional time-delayed feedback for such class of resultant nonlinear system are scarce (to the best of the authors' knowledge and information). The present study is therefore motivated by the need for a better semi-analytical prediction of complex periodic via fast Fourier transform based incremental harmonic balance method along with a continuation technique (IHB-FFTC). Since the system or the feedback control law (which will be developed and introduced in the feedback path) is strongly non-linear, the efficiency of the method to study the response and stability of such system is attempted. The stability of the periodic solution is examined by Floquet theory. The results show that the response curve can be suppressed to the desired level with appropriate choice of delay and gain parameters.

2 Fast Fourier Transform Based Incremental Harmonic Balance Method for Time-Delayed Feedback Systems

2.1 Fourier discretization

Consider the set of non-linear ordinary deferential equations for a multi degree of freedom dynamical system with time-delay of the following general form

$$\phi(t) = \phi(\ddot{x}, \dot{x}, x, x_d, \omega, f, d, t) = 0 \tag{1}$$

With the periodic conditions

$$x(t) = x(t + 2h\pi),\ \dot{x}(t) = \dot{x}(t + 2h\pi),\ \text{and}\ \ddot{x}(t) = \ddot{x}(t + 2h\pi) \tag{2}$$

In this vector equation, ϕ is analytic, $x(t)$ is the unknown response of the non-linear system, or in general, the dependent variable vector, $x_d(t)$ is the time-delayed function, ω is the non-dimensional excitation frequency, d is the time-delay, and f is the external harmonic excitation amplitude. Over dots denote derivatives with respect to the non-dimensional time t and h is the integer order of the sub-harmonic response being considered.

The first step of the IHB method is the Newton–Raphson iterative procedure. To obtain a periodic solution of Eq. (1) one needs to guess a solution at the beginning of the procedure which may be taken as the solution of linear system. A neighboring solution can be expressed by adding the corresponding increments (symbolized by Δ) to them as follows,

$$\phi \to \phi + \Delta\phi,\ x \to x + \Delta x,\ x_d \to x_d + \Delta x_d,\ \omega \to \omega + \Delta\omega\ \text{and}\ f \to f + \Delta f \tag{3}$$

Thus, the left side variables of Eq. (3) can be regarded as the neighbouring states while that on the right side as the sum of known states and their increments. Substituting Eq. (3) into Eq. (1) one obtains the following incremental equation:

$$\phi(t) = \phi(\ddot{x} + \Delta\ddot{x}, \dot{x} + \Delta\dot{x}, x + \Delta x, x_d + \Delta x_d, \omega + \Delta\omega, f + \Delta f, d, t) = 0 \tag{4}$$

Now expanding Eq. (4) by Taylor's series about the initial state up to the first order, the linearized incremental equations are obtained as,

$$\frac{\partial\phi}{\partial\ddot{x}}\Delta\ddot{x} + \frac{\partial\phi}{\partial\dot{x}}\Delta\dot{x} + \frac{\partial\phi}{\partial x}\Delta x + \frac{\partial\phi}{\partial x_d}\Delta x_d + \frac{\partial\phi}{\partial\omega}\Delta\omega + \frac{\partial\phi}{\partial f}\Delta f + \phi(t) = 0 \tag{5}$$

Here $\phi(t)$ is the residue or corrective term which will vanish when the solution is exact. Now replace

$$\frac{\partial\phi}{\partial\ddot{x}} = M,\ \frac{\partial\phi}{\partial\dot{x}} = C,\ \frac{\partial\phi}{\partial x} = K,\ \frac{\partial\phi}{\partial x_d} = D,\ \frac{\partial\phi}{\partial\omega} = W\ \text{and}\ \frac{\partial\phi}{\partial f} = F \tag{6}$$

With these, Eq. (5) takes the form

$$M\Delta\ddot{x} + C\Delta\dot{x} + K\Delta x + D\Delta x_d + W\Delta\omega + F\Delta f + \phi(t) = 0 \quad (7)$$

The terms M, C, K, D, W and F can in general be time (t) varying and are called the equivalent incremental mass, damping, stiffness, delay, frequency and excitation respectively. Eq. (5) or (7) represents a set of linear, second order, variable coefficient, ordinary differential equations (ODEs). The second step of the IHB method is to expand the generalized coordinate $x(t)$ and the corresponding increment $\Delta x(t)$ into Fourier series for periodic response.

$$\begin{Bmatrix} x(t) \\ \Delta x(t) \end{Bmatrix} = \frac{1}{2}\begin{Bmatrix} a_0 \\ \Delta a_0 \end{Bmatrix} + \sum_{i=1}^{\infty}\left(\begin{Bmatrix} a_i \\ \Delta a_i \end{Bmatrix}\cos\frac{it}{h} + \begin{Bmatrix} b_i \\ \Delta b_i \end{Bmatrix}\sin\frac{it}{h} \right) \quad (8a)$$

$$\begin{Bmatrix} x(t) \\ \Delta x(t) \end{Bmatrix} = \begin{Bmatrix} \mathbf{YA} \\ \mathbf{Y}\Delta\mathbf{A} \end{Bmatrix}, \quad (8b)$$

where i denotes any positive integer and

$$\mathbf{Y} = \left[1 \quad \cos\left(\frac{t}{h}\right) \cos\left(\frac{2t}{h}\right) \ldots \cos\left(\frac{it}{h}\right) \ldots \quad \sin\left(\frac{t}{h}\right) \sin\left(\frac{2t}{h}\right) \ldots \sin\left(\frac{it}{h}\right) \ldots \right] \quad (8c)$$

Or $\mathbf{Y} = [1 \quad c_i \quad s_i]$, (8$d$)

where $c_i = \cos\left(\frac{it}{h}\right)$ and $s_i = \sin\left(\frac{it}{h}\right)$

$$\mathbf{A} = \left[\frac{a_0}{2} \quad a_1 \quad a_2 \ldots a_i \ldots b_1 \quad b_2 \ldots b_i \quad \ldots \right] \quad (8e)$$

and

$$\Delta\mathbf{A} = \left[\frac{\Delta a_0}{2} \quad \Delta a_1 \quad \Delta a_2 \ldots \Delta a_i \ldots \quad \Delta b_i \ldots \Delta b_1 \quad \Delta b_2 \ldots \Delta b_i \ldots \right]^{\mathrm{T}} \quad (8f)$$

Here, the upper subscript symbol 'T' denotes the transpose of a matrix. These solutions include all harmonics up to a certain order n and have sub-harmonic order h. From now on it is assumed that $x(t)$ is an approximately known solution and $\Delta x(t)$ is to be found such that $x(t) + \Delta x(t)$ is a new solution. Therefore all functions of time in (6) are known for given $x(t)$ and they can be correlated by expanding using Fourier series as follows:

$$\begin{Bmatrix} M(t) \\ C(t) \end{Bmatrix} = \frac{1}{2}\begin{Bmatrix} M_0 \\ C_0 \end{Bmatrix} + \sum_{u=1}^{\infty}\left[\begin{Bmatrix} M_u^c \\ C_u^c \end{Bmatrix}\cos\frac{ut}{h} + \begin{Bmatrix} M_u^s \\ C_u^s \end{Bmatrix}\sin\frac{ut}{h} \right] \quad (9a)$$

$$\begin{Bmatrix} K(t) \\ D(t) \end{Bmatrix} = \frac{1}{2}\begin{Bmatrix} K_0 \\ D_0 \end{Bmatrix} + \sum_{u=1}^{\infty}\left[\begin{Bmatrix} K_u^c \\ D_u^c \end{Bmatrix}\cos\frac{ut}{h} + \begin{Bmatrix} K_u^s \\ D_u^s \end{Bmatrix}\sin\frac{ut}{h} \right], \quad (9b)$$

and

$$\begin{Bmatrix} W(t) \\ F(t) \\ \phi(t) \end{Bmatrix} = \frac{1}{2}\begin{Bmatrix} W_0 \\ F_0 \\ \phi_0 \end{Bmatrix} + \sum_{u=1}^{\infty}\left[\begin{Bmatrix} W_u^c \\ F_u^c \\ \phi_u^c \end{Bmatrix}\cos\frac{ut}{h} + \begin{Bmatrix} W_u^s \\ F_u^s \\ \phi_u^s \end{Bmatrix}\sin\frac{ut}{h} \right] \quad (9c)$$

Now, the Fourier coefficients of these functions can be calculated most efficiently by applying FFT (fast Fourier transform) algorithm. Considering x_d as the time-delayed displacement of the form $x_d(t) = x(t - \omega d)$, the Fourier series of x_d and Δx_d are expressed as:

$$\begin{Bmatrix} x(t-\omega d) \\ \Delta x(t-\omega d) \end{Bmatrix} = \frac{1}{2}\begin{Bmatrix} a_0 \\ \Delta a_0 \end{Bmatrix} + \sum_{i=1}^{\infty}\left[\begin{Bmatrix} a_i \\ \Delta a_i \end{Bmatrix}\cos\frac{i(t-\omega d)}{h} + \begin{Bmatrix} b_i \\ \Delta b_i \end{Bmatrix}\sin\frac{i(t-\omega d)}{h} \right] \quad (10)$$

Substituting Eq. (8a), (9) and (10) into Eq. (5), we obtain the following linear matrix equation for the unknown increment $\{\Delta A\}$,

$$\{\mathbf{Y}(t)\}\left([\overline{\mathbf{M}} + \overline{\mathbf{C}} + \overline{\mathbf{K}} + \overline{\mathbf{D}}]\{\Delta\mathbf{A}\} + \{\overline{\mathbf{W}}\}\Delta\omega + \{\overline{\mathbf{F}}\}\Delta f + \{\overline{\mathbf{\Phi}}\} \right) = \{\mathbf{0}\} \quad (11a)$$

Where,

$$\overline{\mathbf{W}} = \left[W_0/2 \quad W_1^c \quad W_2^c \quad \ldots \quad W_u^c \quad \ldots \quad W_1^s \quad W_2^s \quad \ldots \quad W_u^s \quad \ldots \right]^{\mathrm{T}}, \quad (11b)$$

and

$$\overline{\mathbf{F}} = [F_0/2 \quad F_1^c \quad F_2^c \quad \ldots \quad F_u^c \quad \ldots \quad F_1^s \quad F_2^s \quad \ldots \quad F_u^s \quad \ldots]^{\mathrm{T}} \quad (11c)$$

Let us define $[\mathbf{J}] = [\overline{\mathbf{M}} + \overline{\mathbf{C}} + \overline{\mathbf{K}} + \overline{\mathbf{D}}]$ as the Jacobian (gradient or tangential) matrix with respect to $\{\Delta A\}$ in which the matrices $[\overline{\mathbf{M}}]$, $[\overline{\mathbf{C}}]$, $[\overline{\mathbf{K}}]$ and $[\overline{\mathbf{D}}]$ are defined by as

$$\{\mathbf{Y}(t)\}[\overline{\mathbf{M}}][\Delta\mathbf{A}] = M(t)\Delta\ddot{x}, \quad (12a)$$

$$\{\mathbf{Y}(t)\}[\overline{\mathbf{C}}][\Delta\mathbf{A}] = C(t)\Delta\dot{x}, \quad (12b)$$

$$\{\mathbf{Y}(t)\}[\overline{\mathbf{K}}][\Delta\mathbf{A}] = K(t)\Delta x, \quad (12c)$$

and

$$\{\mathbf{Y}(t)\}[\overline{\mathbf{D}}][\Delta\mathbf{A}] = D(t)\Delta x(t - \omega d) \quad (12d)$$

2.2 Evaluation of Jacobian matrix

The elements of the Jacobian matrix in Eq. (12) are effectively calculated using FFT method. Here we will evaluate only $[\overline{\mathbf{D}}]$ in detail. The results for $[\overline{\mathbf{C}}]$, $[\overline{\mathbf{K}}]$ and $[\overline{\mathbf{M}}]$ are supplied directly from Leung and Chui (1995), [15].The elements of $[\overline{\mathbf{D}}]$ in terms of Fourier components of $D(t)$ are expressed as,

$$[\overline{\mathbf{D}}]=\begin{bmatrix} D_{00} & D_{0j}^{c} & D_{0j}^{s} \\ D_{i0}^{c} & D_{ij}^{cc} & D_{ij}^{cs} \\ D_{i0}^{s} & D_{ij}^{sc} & D_{ij}^{ss} \end{bmatrix} \tag{13}$$

From Eq. (12*d*),

$$\begin{bmatrix} 1 & c_i & s_i \end{bmatrix}\begin{bmatrix} D_{00} & D_{0j}^{c} & D_{0j}^{s} \\ D_{i0}^{c} & D_{ij}^{cc} & D_{ij}^{cs} \\ D_{i0}^{s} & D_{ij}^{sc} & D_{ij}^{ss} \end{bmatrix}\begin{bmatrix} \Delta a_0 \\ \Delta a_i \\ \Delta a_i \end{bmatrix}$$

$$=\left[\frac{D_0}{2}+\sum_{u=1}^{\infty}\left(D_u^c c_u+D_u^s s_u\right)\right]$$

$$\left[\frac{\Delta a_0}{2}+\sum_{j=1}^{\infty}\left\{\Delta a_j\left(c_j\cos\frac{j\omega d}{h}+s_j\sin\frac{j\omega d}{h}\right)\right.\right.$$

$$\left.\left.+\Delta b_j\left(s_j\cos\frac{j\omega d}{h}+c_j\sin\frac{j\omega d}{h}\right)\right\}\right] \tag{14}$$

where D_0, D_u^c and D_u^s are the Fourier coefficients of $D(t)$.

(*i*).Equating first the coefficients of Δa_0 on both side of Eq. (14), we obtain,

$$\begin{bmatrix} 1 & c_i & s_i \end{bmatrix}\begin{bmatrix} D_{00} \\ D_{i0}^{c} \\ D_{i0}^{s} \end{bmatrix}=\frac{1}{2}\left[\frac{D_0}{2}+\sum_{u=1}^{\infty}\left(D_u^c c_u+D_u^s s_u\right)\right] \tag{15}$$

This implies,

$$D_{00}=\frac{1}{4}D_0,\ D_{i0}^{c}=\frac{1}{2}D_i^c,\ \text{and}\ D_{i0}^{s}=\frac{1}{2}D_i^s$$

(*ii*) Next, evaluate the coefficient of Δa_j on both sides of Eq. (14) for a certain *j*.

$$\begin{bmatrix} 1 & c_i & s_i \end{bmatrix}\begin{bmatrix} D_{0j}^{c} \\ D_{ij}^{cc} \\ D_{ij}^{sc} \end{bmatrix}=\left[\frac{D_0}{2}+\sum_{u=1}^{\infty}\left(D_u^c c_u+D_u^s s_u\right)\right]$$

$$\left(c_j\cos\frac{j\omega d}{h}+s_j\sin\frac{j\omega d}{h}\right) \tag{16a}$$

$$\begin{bmatrix} 1 & c_i & s_i \end{bmatrix}\begin{bmatrix} D_{0j}^{c} \\ D_{ij}^{cc} \\ D_{ij}^{sc} \end{bmatrix}$$

$$=\cos\left(\frac{j\omega d}{h}\right)\left[\frac{D_0}{2}+\sum_{u=1}^{\infty}\left(D_u^c c_u+D_u^s s_u\right)\right]c_j$$

$$+\sin\left(\frac{j\omega d}{h}\right)\left[\frac{D_0}{2}+\sum_{u=1}^{\infty}\left(D_u^c c_u+D_u^s s_u\right)\right]s_j \tag{16b}$$

Next, we apply Galerkin's method or the harmonic balance method to evaluate the Fourier coefficients. Multiplying both sides of the above equation by c_i and s_i, respectively and integrating over time *t* from zero to $2\pi h$ and then equate it to zero, we have respectively,

$$\int_0^{2h\pi} c_i\begin{bmatrix} 1 & c_i & s_i \end{bmatrix}\begin{bmatrix} D_{0j}^{c} \\ D_{ij}^{cc} \\ D_{ij}^{sc} \end{bmatrix}dt$$

$$=\cos\left(\frac{j\omega d}{h}\right)\int_0^{2h\pi}\left(\frac{D_0}{2}+\sum_{u=1}^{\infty}\left[D_u^c c_u+D_u^s s_u\right]\right)c_i c_j dt$$

$$+\sin\left(\frac{j\omega d}{h}\right)\int_0^{2h\pi}\left(\frac{D_0}{2}+\sum_{u=1}^{\infty}\left[D_u^c c_u+D_u^s s_u\right]\right)c_i s_j dt, \tag{17}$$

and

$$\int_0^{2h\pi} s_i\begin{bmatrix} 1 & c_i & s_i \end{bmatrix}\begin{bmatrix} D_{0j}^{c} \\ D_{ij}^{cc} \\ D_{ij}^{sc} \end{bmatrix}dt$$

$$=\cos(j\omega d/h)\int_0^{2h\pi}\left(\frac{D_0}{2}+\sum_{u=1}^{\infty}\left[D_u^c c_u+D_u^s s_u\right]\right)s_i c_j dt$$

$$+\ \sin(j\omega d/h)\int_0^{2h\pi}\left(\frac{D_0}{2}+\sum_{u=1}^{\infty}\left[D_u^c c_u+D_u^s s_u\right]\right)s_i s_j dt \tag{18}$$

Use of the following general trigonometric relations and orthogonality relations between sine and cosine functions are helpful to simplify Eq. (17) and (18). Here *q* and *r* are zero or integers.

$$s_q c_r=\frac{1}{2}\left(s_{q+r}+s_{q-r}\right) \tag{19a}$$

$$c_q c_r=\frac{1}{2}\left(c_{q+r}+c_{q-r}\right) \tag{19b}$$

$$s_q s_r=-\frac{1}{2}\left(c_{q+r}-c_{q-r}\right) \tag{19c}$$

$$\int_0^{2h\pi} s_q c_r dt=0 \quad \text{for all } q \text{ and } r \tag{19d}$$

$$\int_0^{2h\pi} s_q s_r dt = \begin{cases} h\pi & \text{for } q = r \\ 0 & \text{for } q \neq r \end{cases} \quad (19e)$$

$$\int_0^{2h\pi} c_q c_r dt = \begin{cases} 2h\pi & \text{for } q = r = 0 \\ h\pi & \text{for } q = r \neq 0 \\ 0 & \text{for } q \neq r \end{cases} \quad (19f)$$

Therefore, for the cosine terms we have,

$$h\pi D_{ij}^{cc} = \cos\left(\frac{j\omega d}{h}\right) \int_0^{2h\pi} \left(\frac{D_0}{2} + \sum_{u=1}^{\infty} \left[D_u^c c_u + D_u^s s_u\right]\right)$$

$$\left(\frac{1}{2}\right)(c_{i+j} + c_{i-j})dt$$

$$+ \sin(j\omega d / h) \int_0^{2h\pi} \left(\frac{D_0}{2} + \sum_{u=1}^{\infty} \left[D_u^c c_u + D_u^s s_u\right]\right)$$

$$\left(\frac{1}{2}\right)(s_{i+j} - s_{i-j})dt \quad (20)$$

A similar expression can be obtained for sine terms and not shown to maintain brevity. Finally, from Eq. (17) and (18) we obtain,

$$D_{0j}^c = \frac{1}{2}\left[\cos\left(\frac{j\omega d}{h}\right) D_i^c + \frac{1}{2}\sin\left(\frac{j\omega d}{h}\right) D_i^s\right] \text{ for } i = 0 \quad (21a)$$

$$D_{ij}^{cc} = \frac{1}{2}\left[\cos\left(\frac{j\omega d}{h}\right)\left(\mathrm{D}_{i+j}^c + D_{|i-j|}^c\right)\right.$$

$$\left. + \cos\left(\frac{j\omega d}{h}\right)\left(D_{i+j}^s - \text{sgn}(i-j) D_{|i-j|}^s\right)\right] \text{ for } i \neq 0 \quad (21b)$$

$$D_{ij}^{sc} = \frac{1}{2}\left[\cos\left(\frac{j\omega d}{h}\right)\frac{j\omega d}{h}\left(D_{i+j}^s + \text{sgn}(i-j) D_{|i-j|}^s\right)\right.$$

$$\left. + \sin\left(\frac{j\omega d}{h}\right)\left(D_{|i-j|}^c - \mathrm{D}_{i+j}^c\right)\right] \text{ for all } i \quad (21c)$$

(*iii*) Next we equate the coefficient of Δb_j on both sides of Eq. (14) for a certain *j*.

$$[1 \;\; c_i \;\; s_i] \begin{bmatrix} D_{0j}^s \\ D_{ij}^{cs} \\ D_{ij}^{ss} \end{bmatrix} = \left[\frac{D_0}{2} + \sum_{u=1}^{\infty}\left(D_u^c c_u + D_u^s s_u\right)\right]$$

$$\left[s_j \cos\left(\frac{j\omega\omega}{h}\right) + c_j \sin\left(\frac{j\omega\omega}{h}\right)\right] \quad (22a)$$

$$[1 \;\; c_i \;\; s_i] \begin{bmatrix} D_{0j}^s \\ D_{ij}^{cs} \\ D_{ij}^{ss} \end{bmatrix}$$

$$= \cos\left(\frac{j\omega d}{h}\right)\left(\frac{D_0}{2} + \sum_{u=1}^{\infty}\left[D_u^c c_u + D_u^s s_u\right]\right) s_j$$

$$- \sin\left(\frac{j\omega d}{h}\right)\left(\frac{D_0}{2} + \sum_{u=1}^{\infty}\left[D_u^c c_u + D_u^s s_u\right]\right) c_j \quad (22b)$$

Applying the harmonic balance method as above we obtain,

$$D_{0j}^s = \frac{1}{2}\left[\cos\left(\frac{j\omega d}{h}\right) D_j^s - \sin\left(\frac{j\omega d}{h}\right) D_j^c\right] \quad (23a)$$

$$D_{ij}^{cs} = \frac{1}{2}\left[\cos\left(\frac{j\omega d}{h}\right)\left(D_{i+j}^s - \text{sgn}(i-j) D_{|i-j|}^s\right)\right.$$

$$\left. - \sin\left(\frac{j\omega d}{h}\right)\left(D_{i+j}^c - D_{|i-j|}^c\right)\right], \quad (23b)$$

and

$$D_{ij}^{ss} = \frac{1}{2}\left[\cos\left(\frac{j\omega d}{h}\right)\left(D_{|i-j|}^c - D_{i+j}^c\right)\right.$$

$$\left. - \sin\left(\frac{j\omega d}{h}\right)\left(D_{i+j}^s + \text{sgn(i - j)} \mathrm{D}_{|i-j|}^s\right)\right] \quad (23c)$$

The elements of $[\overline{\mathbf{M}}]$ in terms of Fourier components of $M(t)$ are expressed as,

$$[\overline{\mathbf{M}}] = \begin{bmatrix} M_{00} & M_{0j}^c & M_{0j}^s \\ M_{i0}^c & M_{ij}^{cc} & M_{ij}^{cs} \\ M_{i0}^s & M_{ij}^{sc} & M_{ij}^{ss} \end{bmatrix}, \quad (24)$$

where,

$$M_{00} = M_{i0}^c = M_{i0}^s = 0, \quad (25a)$$

$$M_{0j}^c = -\left(\frac{j^2}{2h^2}\right) M_j^c, \quad (25b)$$

$$M_{ij}^{cc} = -\left(\frac{j^2}{2h^2}\right)\left(M_{i+j}^c + M_{|i-j|}^c\right), \quad (25c)$$

$$M_{ij}^{sc} = -\left(\frac{j^2}{2h^2}\right)\left(M_{i+j}^c + \text{sgn}(i-j) M_{|i-j|}^s\right) \text{ for } i \neq 0, \quad (25d)$$

$$M_{0j}^s = -\left(\frac{j^2}{2h^2}\right) M_j^s, \quad (25e)$$

$$M_{ij}^{cs} = -\left(\frac{j^2}{2h^2}\right)\left(M_{i+j}^s - \text{sgn}(i-j) M_{|i-j|}^s\right), \quad (25f)$$

and

$$M_{ij}^{ss} = -\left(\frac{j^2}{2h^2}\right)\left(M_{|i-j|}^c - M_{i+j}^c\right) \text{ for } i \neq 0 \quad (25g)$$

The elements of $[\overline{\mathbf{C}}]$ in terms of Fourier components of $C(t)$ are expressed as,

$$[\overline{\mathbf{C}}]=\begin{bmatrix} C_{00} & C_{0j}^{c} & C_{0j}^{s} \\ C_{i0}^{c} & C_{ij}^{cc} & C_{ij}^{cs} \\ C_{i0}^{s} & C_{ij}^{sc} & C_{ij}^{ss} \end{bmatrix}, \quad (26)$$

where,

$$C_{00}=C_{i0}^{c}=C_{i0}^{s}=0, \quad (27a)$$

$$C_{0j}^{c}=-\frac{j}{2h}C_{j}^{s} \text{ for} i=0, \quad (27b)$$

$$C_{ij}^{cc}=-\frac{1}{2h}\left(C_{i+j}^{s}-\text{sgn}(i-j)C_{|i-j|}^{s}\right) \text{for} i\neq 0, \quad (27c)$$

$$C_{ij}^{sc}=-\frac{1}{2h}\left(C_{|i-j|}^{c}-C_{i+j}^{c}\right) \text{for all } i, \quad (27d)$$

$$C_{0j}^{s}=\frac{j}{2h}C_{j}^{c}, \quad (27e)$$

$$C_{ij}^{cs}=\frac{1}{2h}\left(C_{i+j}^{c}+C_{|i-j|}^{c}\right), \quad (27f)$$

and

$$C_{ij}^{ss}=\frac{1}{2h}\left(C_{i+j}^{s}+\text{sgn}(i-j)C_{|i-j|}^{s}\right) \text{ for} i\neq 0. \quad (27g)$$

The elements of $[\overline{\mathbf{K}}]$ in terms of Fourier components of $K(t)$ are expressed as,

$$[\overline{\mathbf{K}}]=\begin{bmatrix} K_{00} & K_{0j}^{c} & K_{0j}^{s} \\ K_{i0}^{c} & K_{ij}^{cc} & K_{ij}^{cs} \\ K_{i0}^{s} & K_{ij}^{sc} & K_{ij}^{ss} \end{bmatrix} \quad (28)$$

Where $K_{00}=\frac{1}{4}K_0$, $K_{i0}^{c}=\frac{1}{2}K_i^{c}$, $K_{i0}^{s}=\frac{1}{2}K_i^{s}$,

$K_{0j}^{c}=-\frac{1}{2}\mathrm{K_j^c}$, $K_{ij}^{cc}=\frac{1}{2}\left(\mathrm{K_{i+j}^c}+K_{|i-j|}^{c}\right)$

$K_{ij}^{sc}=\frac{1}{2}\left(\mathrm{K_{i+j}^s}+\text{sgn}(i-j)K_{|i-j|}^{s}\right)$ for $i\neq 0$,

$K_{0j}^{s}=\frac{1}{2}K_j^{s}$, $K_{ij}^{cs}=\frac{1}{2}\left(K_{i+j}^{s}-\text{sgn}(i-j)K_{|i-j|}^{s}\right)$,

and $K_{ij}^{ss}=\frac{1}{2}\left(\mathrm{K_{|i-j|}^c}-K_{i+j}^{c}\right)$ for $i\neq 0$

Next $\{\overline{\mathbf{W}}\}$, $\{\overline{\mathbf{F}}\}$ and $\{\overline{\mathbf{\Phi}}\}$ in Eq. (11*a*) are calculated using FFT algorithm and it is solved for the unknown coefficient vector $\{\Delta\mathbf{A}\}$.

Finally, the matrix Eq. (11*a*) is solved at each time step using the Newton-Rapson iterative process.

2.3 Path following and parametric continuation

The FFT-IHB method with a variable parameter is ideally suited to parametric continuation for obtaining the response diagrams of nonlinear systems. After obtaining the solution for the particular value of a parameter, the solution for a new parameter slightly perturbed from the old one can be obtained by iterations using the previous solution as an approximation. The main aim of the path following and parametric continuation is to effectively trace the bifurcation sequence as a parameter of the system is varied. In this study, an arc length procedure[16] is adopted for the parametric continuation.

Introducing the path parameterγ, the augmenting equation for a general system can be written as:

$$\varphi(\mathbf{X})-\gamma=0 \quad (29)$$

where $\{\mathbf{X}\}=[\{\mathbf{A}\}^{\mathrm{T}},\omega]^{T}$. A good choice of the function $g\{\mathbf{X}\}$ is $g(\mathbf{X})=\{\mathbf{X}\}^{T}\{\mathbf{X}\}$. Considering the increments in $\{\mathbf{A}\}$, F and γ, the incremental equation is obtained as

$$\frac{\partial\varphi}{\partial\mathbf{A}^{\mathrm{T}}}\{\Delta\mathbf{A}\}+\frac{\partial\varphi}{\partial\omega}\Delta\omega-\Delta\gamma+\varphi-\gamma=0 \quad (30)$$

Together with (11), we obtain the augmented incremented incremental equation

$$\{\mathbf{Y}(t)\}\left([\overline{\mathbf{M}}+\overline{\mathbf{C}}+\overline{\mathbf{K}}+\overline{\mathbf{D}}]\{\Delta\mathbf{A}\}+\{\overline{\mathbf{W}}\}\Delta\omega+\{\overline{\mathbf{\Phi}}\}+\{\overline{\mathbf{F}}\}\Delta f+\{\overline{\mathbf{\Phi}}\}\right)=\{\mathbf{0}\} \quad (31)$$

$$[\mathbf{J_X}]\{\Delta\mathbf{X}\}=\begin{bmatrix} [\mathbf{J}] & \overline{\mathbf{W}} \\ \left\{\frac{\partial\varphi}{\partial\mathbf{A}}\right\}^{T} & \left\{\frac{\partial\varphi}{\partial\omega}\right\} \end{bmatrix}\begin{Bmatrix}\Delta\mathbf{A}\\ \Delta\omega\end{Bmatrix}=-\begin{Bmatrix}\overline{\mathbf{\Phi}}\\ \varphi-\gamma-\Delta\gamma\end{Bmatrix} \quad (32)$$

where $[\mathbf{J}]=[\overline{\mathbf{M}}+\overline{\mathbf{C}}+\overline{\mathbf{K}}+\overline{\mathbf{D}}]$ as before, and $[\mathbf{J_X}]$ is the Jacobian matrix which is modified with respect to $\{\mathbf{X}\}$. Considering the portion of the equilibrium path of the solution branch, the augmenting equation can be written as

$$\varphi(\mathbf{X})-\gamma-\{\mathbf{X}'\}^{T}\{\mathbf{X}-\mathbf{X_c}\}=0 \quad (33)$$

The first prediction of the new point $\{\mathbf{X_n}\}$ of the solution along the equilibrium path is given in terms of the two previous points $\{\mathbf{X_c}\}$ and $\{\mathbf{X_{cc}}\}$ as follows:

$$\left.\begin{aligned}\{\mathbf{X_n}\}&=\{\mathbf{X_c}\}+\mathbf{\Delta\gamma}\{\mathbf{X}'\}, \text{ and}\\ \{\mathbf{X}'\}&=\{\mathbf{X_c}-\mathbf{X_{cc}}\}/\parallel\mathbf{X_c}-\mathbf{X_{cc}}\parallel\end{aligned}\right\} \quad (34)$$

where $\Delta\gamma$ is an arbitrary step length taken in the computation by experience.

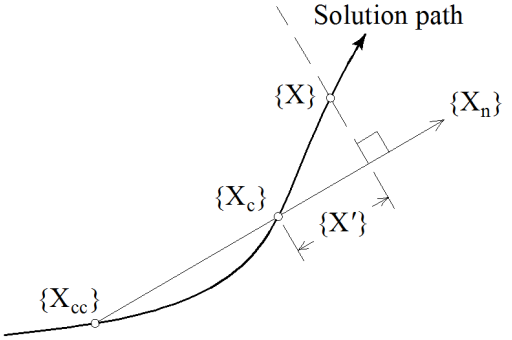

Fig. 1 A portion of the equilibrium path.

2.4 Stability analysis of periodic solutions

When the steady-state solution for time-delay system is computed by using the FFT-IHBC method, the stability of the periodic (or almost periodic) solution is checked by means of Floquet theory for two important reasons. First, stable branches can be distinguished from unstable ones and bifurcation points can be located by monitoring eigenvalues of the monodromy matrix. In this paper Floquet theory is modified to analyse the stability of the periodic solution of time-delayed displacement feedback system. This is done by perturbing the state variables about the steady-state solution, which results in a system of linearized equations with periodically varying coefficients. The perturbed equation of motion is always autonomous. When the solution is perturbed by $\{\Delta x\}$, the incremental linear matrix ordinary differential equation is

$$M\{\Delta\ddot{x}\}+C\{\Delta\dot{x}\}+K\{\Delta x\}+D\{\Delta x_d\}=0 \quad (35)$$

In state space form Eq. (30) can be written as

$$\frac{d}{dt}\begin{bmatrix}\{\Delta x\}\\ \{\Delta\dot{x}\}\end{bmatrix}=\begin{bmatrix}0 & 1\\ -\frac{1}{M}\left(K+D\frac{\dot{x}_d}{\dot{x}}\right) & -\frac{\mathrm{C}}{\mathrm{M}}\end{bmatrix}\begin{Bmatrix}\{\Delta x\}\\ \{\Delta\dot{x}\}\end{Bmatrix} \quad (36)$$

$$\{\dot{z}\}=[\mathbf{B}(t)]\{z\} \quad (37)$$

Where the transition matrix [**B**] is periodic with tine period T, i.e. [B(t)]=[B(t+T)]. The stability of Eq. (32) is checked by evaluating the eigenvalues of the monodromy matrix [**Z**], which transforms the state vector $\{z_n\}$ at $t=nT$ to $\{z_{n+1}\}$ at $t=(n+1)$T. If the absolute magnitudes of the eigenvalues are less than unity, the solution is stable. If at least one of the eigenvalues has a magnitude greater than one, then the periodic solution is unstable. The way the eigenvalues leave the unit circle determines the nature of bifurcations. The explicit form of [**Z**] can be written as [17],

$$[\mathbf{Z}]=\prod_{i=1}^{n}\exp\left(\Delta t[\mathbf{B}(i\Delta t)]\right) \quad (38)$$

where $\Delta t=T/N$, and N represents the number of divisions used to divide one period T. The efficient numerical evaluation [**Z**] is achieved by making use of the definition of the matrix exponential

$$\exp\left(\Delta t[\mathbf{B}]\right)=[\mathbf{I}]+\Delta t[\mathbf{B}]+\frac{\left(\Delta t[\mathbf{B}]\right)^2}{2!}+\ldots+\frac{\left(\Delta t[\mathbf{B}]\right)^n}{n!} \quad (39)$$

where [I] is the identity matrix. For small time intervals $\Delta t\to 0$, the series in equation converges rapidly, and the value of the matrix exponential can be accurately approximated by a finite number of terms.

3. Duffing Oscillator with Time-Delayed Feedback

The Duffing oscillator under mono-harmonic excitation is analysed with time-delayed displacement feedback control. The equation of motion of the system is written as,

$$\omega^2\ddot{x}+\delta\omega\dot{x}+x+\beta x^3=f(t)+g\,x_d, \quad (40)$$

where $x(t)$ is the non-dimensional displacement response as a function of non-dimensional time t. Here t is non-dimensionalized with respect to the natural time period of the oscillator. Dots denote derivatives with respect to t. ω is the non-dimensional excitation frequency. The forcing function is taken as,

$$f(t)=F\cos(t) \quad (41)$$

δ and β denote respectively the damping, non-linear stiffness and parameters. x_d is the control signal and mathematically expressed as

$$x_d=x(t-\omega d) \quad (42)$$

g and d are corresponding gain and delay parameters.

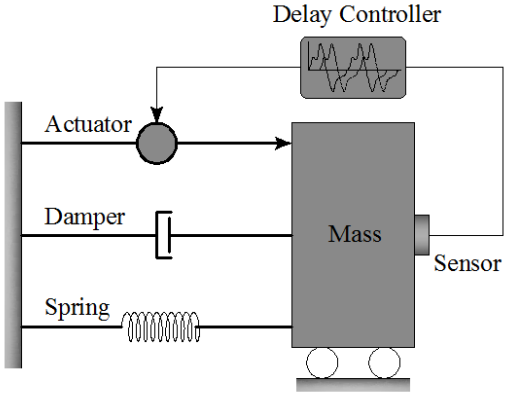

Fig. 2 Time-delayed feedback control scheme of a SDOF mechanical oscillator.

4. Controlling Linear Vibration

4.1 Mathematical model

The non-dimensional equation of motion of the above undamped oscillator with the proposed control is expressed as

$$\omega^2\ddot{x}+x=f(t)+g\,x(t-\omega d) \quad (43)$$

The transfer function (TF) of the linear system governed by Eq.(38) is given by

$$TF=\frac{X(s)}{F(s)}=\frac{1}{\omega^2 s^2+1-ge^{-s\omega d}} \quad (44)$$

Where s is called complex frequency variable. It should be noted that for g=0, Eq.(43) reduces to the transfer function of the uncontrolled system.

4.2 Stability analysis

The stability of the trivial equilibrium of the system is ascertained by the roots of the characteristics equation given below:

$$\omega^2 s^2 + 1 - g e^{-s\omega d} = 0 \quad (45)$$

Substituting $s = j\sigma$ ($j = \sqrt{-1}$ and σ is any real number) in Eq.(45) and separating the imaginary and real parts yields,

$$1 - \omega^2\sigma^2 - g\cos(\sigma\omega d) = 0 \quad (46a)$$

and $$g\sin(\sigma\omega d) = 0 \quad (46b)$$

Since *g* can't be zero,

$$\sin(\sigma\omega d) = 0 \quad (47)$$

The general solution of Eq.(46*b*) is

$$\sigma\omega d = n\pi, \quad \forall n = 0,1,2,...,\infty \quad (48)$$

Substituting Eq.(48) into (46*a*), yields the following equation for the critical stability lines:

$$1 - \left(\frac{n\pi}{d}\right)^2 - g\cos(n\pi) = 0 \quad (49)$$

As the uncontrolled system is marginally stable, $g = 0$ is also a critical stability line. Finally, the stable regions in the *g* vs. *d* plane are obtained from the sign of the root tendency defined below [12],

$$R(\sigma_c, d_c) = \mathrm{sgn}\left[\mathrm{Re}\left(\frac{\mathrm{d}s}{\mathrm{d}d}\bigg|_{(j\sigma_c, d_c)}\right)\right] \quad (50)$$

R	Increase in the number of unstable roots	Decrease in the number of unstable roots
+1	2	
-1		2

Fig.3 depicts the region of stability in the *g* vs. *d* plane. Because the stability region in the lower range of delays is of practical importance, this region is hence forth called as the primary stability zone and the gray shaded regions are called secondary stability zones. In subsequent numerical explorations, parameter values are chosen from the primary as well as secondary stability zones. The negative sign of the control gain in the secondary stability zone establishes the fact that the control system is stable under negative feedback control.

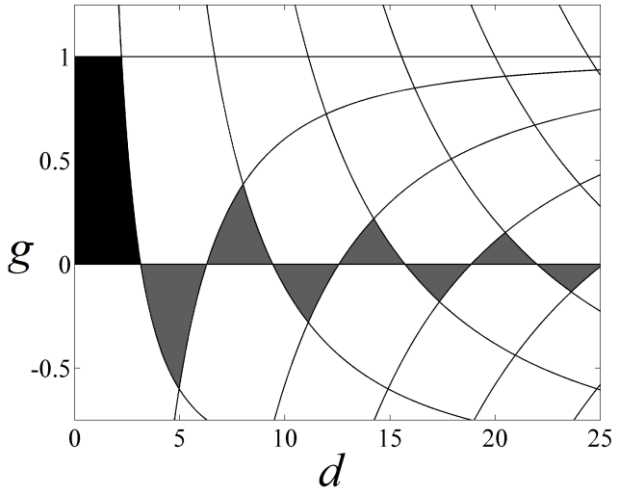

Fig. 3 Stability regions under time-delayed displacement feedback. Shaded regions are stable. Black regions are primary stability zone. Gray regions are secondary stability zones. Solid lines represent the critical stability lines for different *n* on which some of the characteristic roots are purely imaginary.

5. Numerical Discussions

The solutions obtained by FFT-IHBC method for a Duffing oscillator have been presented and compared. Fig. 4 shows the comparison of solutions obtained by FFT-IHBC, phase increment (PI) [18] and numerical integration (NI) method. The Fourier coefficients of damped Duffing oscillator are sourced from Leung and Fung (1989) [18]. The Fourier coefficients obtained at some specific frequencies by PI method is reproduced in Table-1. The Fourier coefficients obtained by FFT-IHBC method for some frequency are listed in Table-2. It should be noted that FFT-IHBC is capable of incorporating a large number of Fourier coefficient for obtaining more accurate solution if necessary. In the table only first six coefficients are given. The amplitude versus frequency plot of the forced Duffing oscillator by FFT-IHBC, NI and PI methods are given in Fig. 4. By PI method the frequency amplitude plot for forced Duffing oscillator has been obtained in the range of 0.9-1.3 rad/s. The frequency response plot for the same oscillator using FFT-IHBC and NI methods, in the present study, is obtained in the range of 0.03-2 rad/s. It is observed from the plot that the FFT-IHBC method traces all branches of possible stable and unstable solutions. A stable branch initiated at 2 rad/s and continues up to an amplitude value of 0.67 m at frequency 1.11 rad/s. From this point stable periodic solution jumps to a peak response value of 1.94 m

through an unstable branch of periodic solution. This jump phenomenon is a typical characteristic of non-linear system. The amplitude of response then reduces sharply and comes down to the amplitude of 0.101 m at frequency 0.09 rad/s. It is observed that the complete resonance curve with stable-unstable-stable branches is developed efficiently by FFT-IHBC method. It is seen from the figure that the discrete points obtained by PI method in the range of 0.9 to 1.3 rad/s matches well with the resonance curve obtained by the present methods (FFT-IHBC and NI). As stated earlier NI method can't provide unstable solution. Also, in Ref. 3 the frequency response curve is developed only for a part of the frequency range with no information about the stability of the solutions obtained.

The forced Duffing oscillator is also investigated for vibration control due to different values of feedback gain and time-delay by both FFT-IHBC and NI methods. Figs. 5 represent frequency response diagrams for different values of gain and delay in the primary stability zone (Fig. 3). Fig. 5*a* represents frequency response curve of the uncontrolled system i.e. g=0 and d=0 s. Figs. 5*b* to 5*d* show the frequency response curves for a constant gain of 0.1 and varying delays. It is observed that there is a continuous reduction in peak value of amplitude as the delay increases. The peak response value has been reduced from 2.72 m to 1.34 m for the said values of gain and delay with proportionate reduction of stable and unstable branches of solution. It may be observed that due to the introduction of gain and delay the frequency response curve shifts to the left indicating an alternation in the natural frequency of the system and in all cases the frequency response curves are associated with the jump phenomena. In Fig. 5*e*, the gain value has been increased to 0.25 with a delay value of 1.5 s. As a result the peak response suppresses appreciably to a value of 0.37 m with all stable solutions and the jump phenomenon vanishes totally. Next in Figs. 5*f* to 5*i*, gain value is fixed at 0.3 and delay values are gradually increased. Here also appreciable reduction in peak response has been achieved. The unstable regions are also reduced. A farther increase of gain to a value of 0.5 and a delay of 0.1 in Fig. 5*j* suppresses the peak response a lot to a value of 0.27m with all stable branches of solutions.

Next, in Fig. 6 the negative gain (-0.25) and a high value of delay (4.75s) values are significantly selected from the secondary stability region of Fig. 3. It is seen that this set of gain and delay results in response curve with all stable solutions.

For all the frequency response curves for different gain and delay values, there is a gradual reduction in peak value of response and skewness of the curves. In case of displacement feedback, Selection of gain and delay values from the other two regions in the secondary stability zone the solutions become unbounded with most unstable solutions. So, in case of displacement feedback, proper selection of gain and delay in the primary and secondary zones can suppress peak response to any desire value.

Table 1. Fourier coefficients obtained by Phase Increment method

ω	a_1	a_2	b_1	b_2
0.96912	0.64457	0.00183	0.17262	0.00177
1.04923	0.91154	0.00204	0.42459	0.00716
1.11679	1.05044	-0.00819	0.73442	0.01327
1.17505	1.06224	-0.01387	1.06011	0.01434
1.22318	0.95929	-0.02447	1.36617	0.00700
1.26041	0.75999	-0.02885	1.62277	-0.00719
1.28625	0.48801	-0.02344	1.80661	-0.02260
1.30049	0.17105	-0.00939	1.90160	-0.03251
1.30314	-0.16062	0.00800	1.89958	-0.03254
1.29440	-0.47583	0.02183	1.80069	-0.02284
1.27479	-0.74426	0.02702	1.61334	-0.40796
1.24525	-0.93812	0.02275	1.35395	0.00544
1.20758	-1.03370	0.01280	1.04629	0.01203
1.16525	-1.01278	0 00331	0.72088	0.01078
1.12572	-0.86524	-0.00118	0.41472	0.00535
1.10783	-0.59733	-0.00100	0.17109	0.00114

Table 2. Fourier coefficients obtained by FFT-IHBC method.

ω	a_1	a_2	a_3	b_1	b_2	b_3
0.17996	0.10313	-0.00010	0.00000	0.00077	-0.00000	0.00000
0.57695	0.14879	0.00010	0.00000	0.00512	0.00000	0.00000
0.96825	0.64178	0.00182	0.00000	0.17085	0.00174	0.00000
1.04894	0.91074	0.00205	-0.00003	0.42347	0.00714	0.00004
1.05296	0.92190	0.00192	-0.00003	0.43958	0.00751	0.00005
1.11504	1.04803	-0.00309	-0.00014	0.72518	0.01315	0.00002
1.17464	1.06245	-0.01379	-0.00019	1.05748	0.01437	-0.00018
1.22177	0.96425	-0.02420	0.00001	1.35657	0.00738	-0.00038
1.26045	0.75963	-0.02887	0.00039	1.62295	-0.00722	-0.00029
1.28563	0.47936	-0.02319	0.00054	1.81094	-0.02304	0.00014
1.30044	0.15382	-0.00852	0.00024	1.90384	-0.03280	0.00054
1.30335	-0.00563	-0.00011	0.00000	1.91271	-0.03389	0.00059
1.29475	-0.46880	0.02161	-0.00050	1.80403	-0.02317	0.00017
1.27456	-0.74662	0.02704	-0.00037	1.61101	-0.00781	-0.00024
1.24566	-0.93648	0.02286	-0.00005	1.35708	0.00532	-0.00033
1.20634	-1.03488	0.01247	0.00014	1.03616	0.01211	-0.00015
1.16538	-1.01290	0.003326	0.00010	0.72136	0.01079	0.00000
1.12633	-0.86806	-0.00116	0.00002	0.41854	0.00543	0.00002
1.10771	-0.58814	-0.00096	-0.00000	0.16545	0.00107	0.00000
1.12272	-0.42780	-0.00042	-0.00000	0.08547	0.00029	0.00000
1.22393	-0.20195	-0.00004	-0.00000	0.02016	0.00001	0.00000
1.43477	-0.09434	-0.00000	-0.00000	0.00512	0.00000	0.00000
1.63167	-0.06009	-0.00000	-0.00000	0.00236	0.00000	0.00000
2.21048	-0.02514	-0.00000	-0.00000	0.00056	0.00000	0.00000

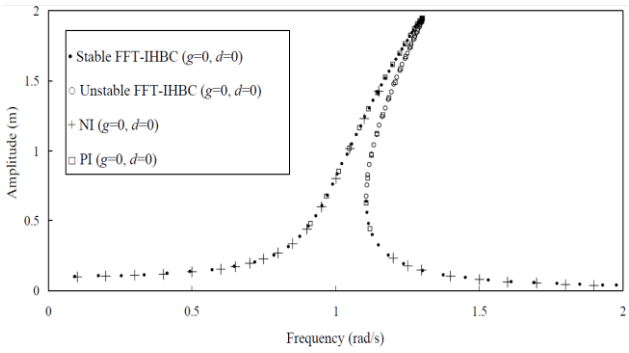

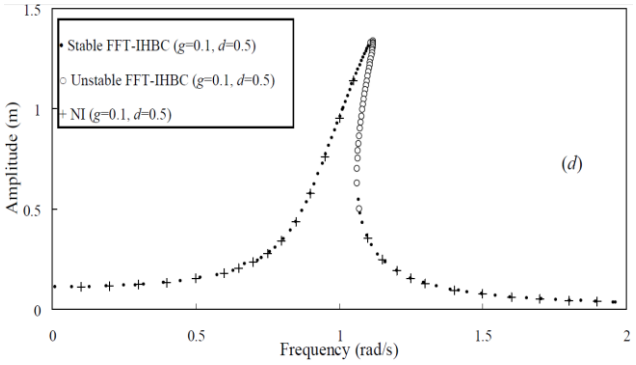

Fig. 4. Frequency response curves of uncontrolled system (δ=0.04, β=0.25, F=0.1, g=0, d=0).

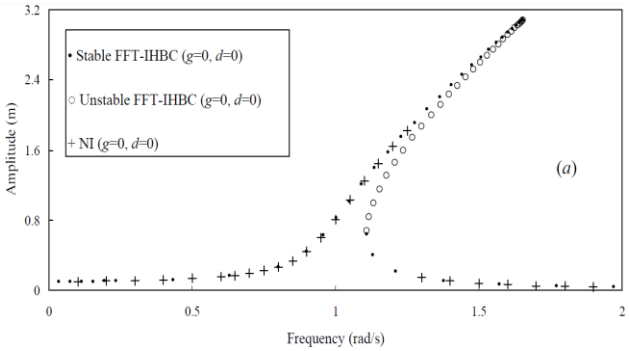

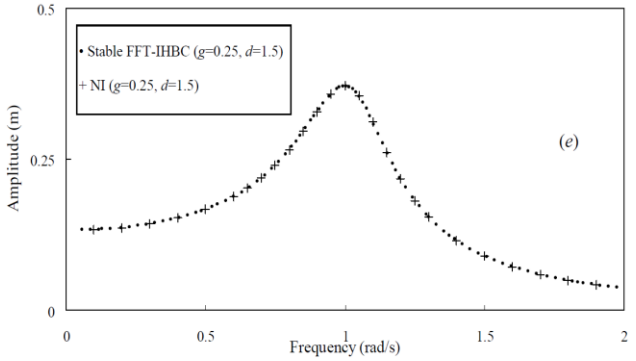

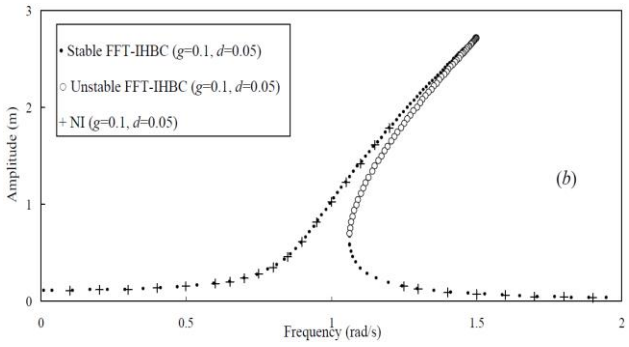

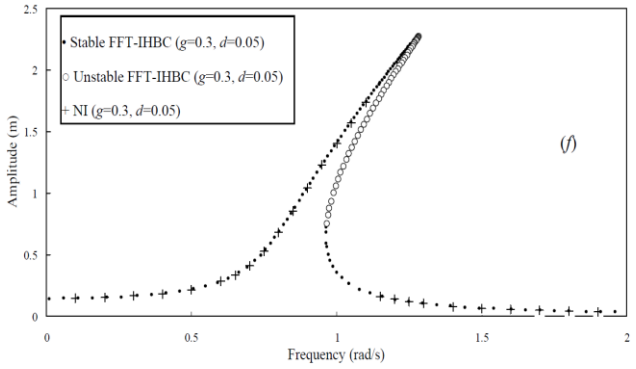

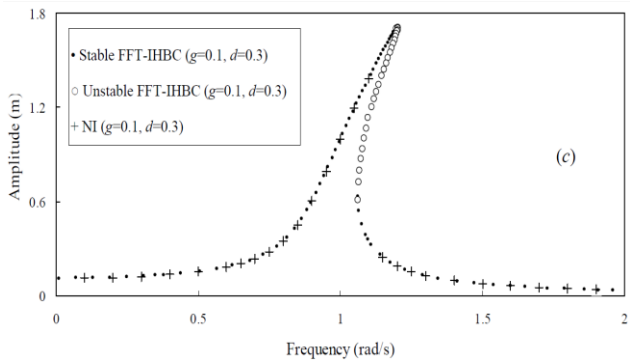

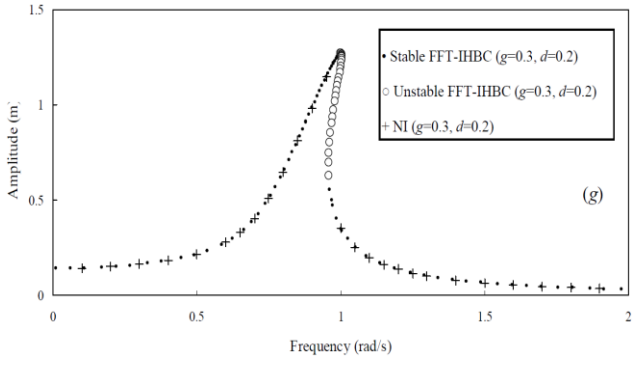

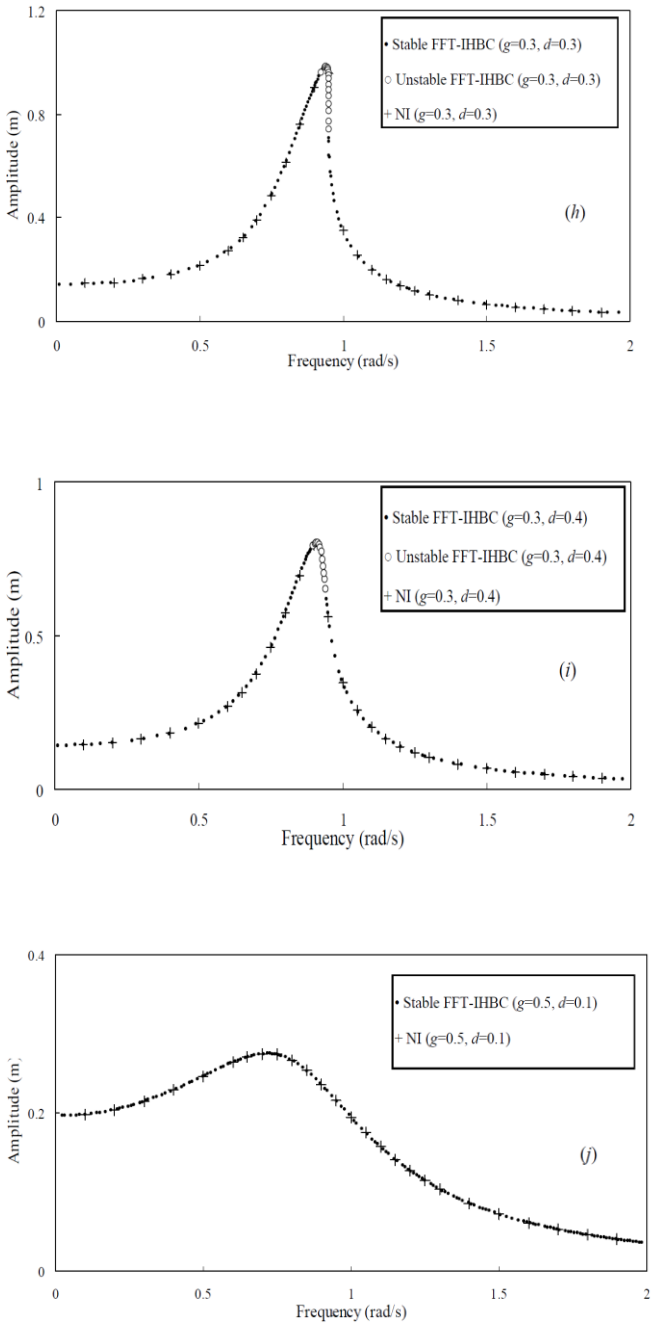

Fig. 5. Frequency response diagram for different gain (positive) and delay in the secondary stability zone (δ=0.02, β=0.25, F=0.1

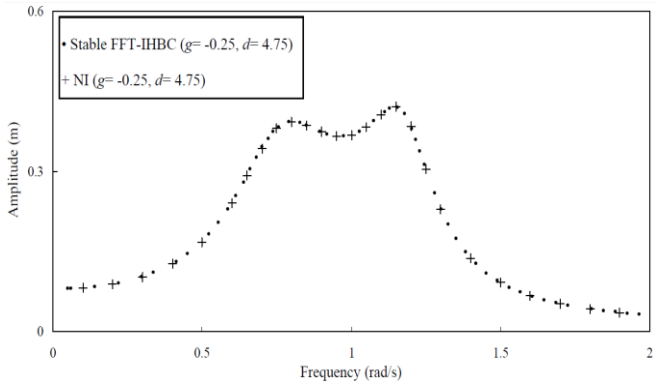

Fig. 6. Frequency response diagrams for gain (negative) and delay in the secondary stability zone (δ=0.02, β =0.25, F=0.1)

6. Conclusions

- The Duffing oscillator under monoharmonic excitation is investigated for desired suppression of peak response by intentional time-delayed displacement feedback. The following conclusions are drawn:
- The computation of Jacobian matrix and hence periodic solution is highly efficient and faster in comparison to simple IHB method.
- A large number of harmonics can be incorporated in FFT-IHBC, if necessary; whereas simple IHB method encounters difficulty with large number of harmonics.
- The solutions obtained by NI matches perfectly with stable solutions obtained by FFT-IHBC method.
- FFT-IHBC can conveniently handle any type of nonlinearity whereas nonlinearity after necessary transformation amenable to IHB method can only be handled by simple IHB method.
- The complete frequency response curve with all possible stable and unstable solution and solution branches can be very efficiently developed by FFT-IHBC method and jump etc. can be observed.
- The introduction of gain delay in the forced Duffing oscillator results in appreciable reduction in the peak value of response.

- For g=0.3 and d=0.4 s all solutions become stable and jump phenomena is no longer observed.

- It is observed that appropriate selection of gain and delay parameters in intentional time-delayed feedback significantly changes the resonances curves and stability of solutions and sometimes in better suppression of vibrations.

References:

[1] K. Gu, and S. Niculescu, Survey on Recent Results in the Stability and Control of Time-delay Systems, ASME Journal of Dynamic Systems, Measurements and Control, 125 (2003) 158-165.

[2] N. Olgac, B.T. Holm-Hansen, A novel active vibration absorption technique: delayed resonator, Journal of Sound and Vibration 176 (1994) 93–104.

[3] N. Jalili, N. Olgac, Multiple identical delayed-resonator vibration absorbers for multi-degree-of freedom mechanical structures, Journal of Dynamic Systems, Measurement, and Control, ASME 122 (2000) 314–322.4.

[4] H. Hu, E.H. Dowell, L.N. Virgin, Resonances of a harmonically forced Duffing oscillator with time-delay state feedback, Nonlinear Dynamics 15 (1998) 311–327.

[5] F.E. Udwadia, H. von Bremen, R. Kumar, M. Hosseini, Time-delayed control of structures, Earthquake Engineering and Structural Dynamics 32 (2003) 495–535.

[6] F.E. Udwadia, H. von Bremen, P. Phohomsiri, Time-delayed control design for active control of structures: principles and application, Structural Control Health Monitoring 12 (3) (2005).

[7] P. Phohomsiri, F.E. Udwadia, H.F. von Bremen, Time-delayed positive velocity feedback control design for active control of structures, Journal of Engineering Mechanics, ASCE (2006) 690–703.

[8] A. Maccari, Vibration control for parametrically excited Lie´nard systems, International Journal of Non-Linear Mechanics 41 (2006) 146–155.

[9] F.M. Atay, Van der Pol's oscillator under delayed feedback, Journal of Sound and Vibration 218 (1998) 333–339.

[10] A. Maccari, Vibration control for the primary resonance of a cantilever beam by a time-delay state feedback, Journal of Sound and Vibration 259 (2003) 241–251.

[11] S. Chatterjee, Time-delayed feedback control of friction induced instabilities, International Journal of Non-Linear Mechanics 42 (9) (2007) 1127–1143.

[12] S. Chatterjee, "Vibration control by recursive time-delayed acceleration feedback", Journal of Sound and Vibration, 317 (2008) 67–90.

[13] Y. M. Ram, A. Singh, and J. E. Mottershead, State feedback control with time-delay", Mechanical Systems and Signal Processing, 23 (2009) 1940–1945.

[14] A. F. El-Bassiouny, and S. El-kholy, Resonances of a non-linear SDOF system with time-delay in linear feedback control", Physica Scripta, 81 (2009) no.1.

[15] A. Y. T. Leung, and S. K. Chui, Non-linear vibration of coupled Duffing oscillator by an improved incremental harmonic balance method, Journal of sound and vibration 181(4), (1995) 619-633.

[16] A. K. Banik, and T. K. Datta, Stability Analysis of Two-Point Mooring System in Surge Oscillation, ASME, Journal of Computational and Nonlinear Dynamics, Vol. 5, 021005-1 (2010).

[17] P. Friedmann, C. E Hammond, and T. H. Woo, Efficient Numerical Treatment of Periodic Systems With Application to Stability Problems, International Journal of Numerical. Methods in Engineering, 11 (1997) 1117–1136.

[18] A. Y. T. Leung, and T. C. Fung, Phase increment analysis of damped Duffing oscillators, Internal Journal of numerical methods in engineering, Vol. 28 (1989).193-209.